

# How to measure a Majorana: The Majorana polarization of a topological planar Josephson junction

Szczepan Głodzik,<sup>\*</sup> Nicholas Sedlmayr,<sup>†</sup> and Tadeusz Domański<sup>‡</sup>  
*Institute of Physics, M. Curie-Skłodowska University, 20-031 Lublin, Poland*  
(Dated: May 23, 2022)

We analyze the topological superconductivity, and investigate the spectroscopic properties manifested by zero-energy modes, induced in a metallic strip embedded into a Josephson-type junction. Focusing on the Majorana polarization of such quasiparticles we propose feasible means for its empirical detection, using the spin selective Andreev reflection method. Our study reveals a gradual development of a transverse gradient of the Majorana polarization across the metallic strip upon increasing its width. We also inspect the spatial profile and polarization of the Majorana quasiparticles in the presence of a strong electrostatic defect. We show that, depending on its position, such a defect can lead to a substantial localization of the Majorana mode.

## I. INTRODUCTION

Topological materials, including those which are either insulators or superconductors, differ qualitatively from their ordinary counterparts due to the emergence of in-gap modes. Such quasiparticles develop at boundaries or internal defects and are topologically protected (thus being good candidates for stable qubits), and obey fractional statistics (which is appealing for quantum computations). Experimental efforts for the realization of these exotic quasiparticles have so far largely focused on one-dimensional structures, e.g. semiconducting nanowires proximitized to superconductors,<sup>1–5</sup> nanochains of magnetic atoms deposited on superconducting substrates,<sup>6–11</sup> and lithographically fabricated nanostructures.<sup>12</sup> Another direction in pursuit of topological superconductivity relies on two-dimensional systems, where the in-gap quasiparticles are chiral modes.<sup>13–17</sup> Such Majorana edge modes have indeed been observed in STM measurements, using nanoscopic islands of magnetic atoms deposited on superconducting substrates.<sup>18–20</sup> Further interesting perspectives are related with mixed-dimensionality systems, where the localized and delocalized Majorana quasiparticles coexist with one another.<sup>21,22</sup> In particular, nanowires attached to larger structures<sup>23</sup> could enable a controllable transfer of the Majorana modes between these constituents,<sup>24</sup> indirectly probing their Chern numbers.<sup>25</sup>

Yet another promising platform for the realization of topological superconductivity hosting localized Majorana modes has been suggested in Refs.<sup>26,27</sup> using metallic strips with strong spin-orbit coupling embedded between two superconducting leads with differing phases (see Fig. 1). Signatures of zero-energy modes have been observed in such heterostructures, consisting both of aluminium on indium arsenide<sup>28</sup> and an HgTe quantum well coupled to thin-film aluminium.<sup>29</sup> The major virtue of a Josephson-type geometry is its tunability to the topologically non-trivial regime, easily controlled experimentally by varying the phase difference. Another way for a controllable transition to the topological phase is possible by using two gate-tunable Josephson junctions

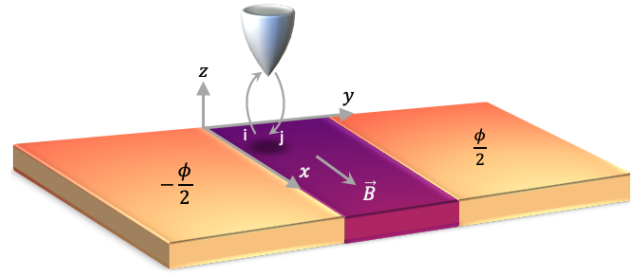


FIG. 1. A schematic view of a metallic strip (dark purple), embedded between superconducting regions (yellow) which differ in phase by  $\phi$ , probed by a polarized STM tip (light gray). A magnetic field  $\vec{B} = B_0\hat{x}$  is applied to the whole structure.

(i.e. a SQUID geometry), as recently reported for epitaxial Al/InAs structures.<sup>30</sup>

Experiments on these Josephson junction heterostructures<sup>28–30</sup> have triggered further intensive studies.<sup>31–34</sup> The proximitized metallic strips are hoped, for instance, to enable a current-controlled braiding of the Majorana modes.<sup>35</sup> It has also been suggested<sup>36</sup> that weak disorder promotes localization of the Majorana quasiparticles.

Intrigued by this prediction, we study here the spatial profiles and polarizations of the Majorana modes. We also consider a single strong point-like electrostatic scattering potential placed in various regions of the proximitized metallic strip. For this purpose we perform numerical calculations within the Bogoliubov-de Gennes treatment. Our study reveals that, when this local defect is placed in an interior of the metallic stripe its influence on the Majorana modes is naturally practically negligible, but when placed near a region of the existing Majorana quasiparticle we observe a tendency towards reducing the spatial extent of the zero-energy modes, in some analogy to what has been predicted by Haim and Stern.<sup>36</sup> These phenomena are in stark contrast to the properties of Majorana quasiparticles of strictly 1-dimensional systems, where sufficiently strong local defects can produce additional pairs of the Majorana modes.

We also inspect the *Majorana polarization* introduced

in Refs. 21, 37–39 and considered by one of us.<sup>40</sup> We show that this quantity could be particularly useful in characterizing the zero-energy quasiparticles of metallic strips whose experimentally reported length-to-width ratio was about 20 (Ref. 28) or 100 (Ref. 29). It is known that quasi 2-dimensionality induces transverse gradients in the Majorana polarization.<sup>21,38,41</sup> Similarly quasi 1-dimensional systems, such as those considered here, can have long localization length scales for the Majorana bound states which can also induce transverse gradients in the Majorana polarization. Strictly the gradient is induced in the phase of the Majorana polarization, and in the magnitude of the Majorana polarization *relative to its density*. We prove that the magnitude (absolute value) can be probed by selective equal spin Andreev reflection spectroscopy.<sup>42</sup> A similar method has previously been applied for inspecting the spin polarization of the Majorana quasiparticles of *Fe* atom chains using a magnetic STM tip.<sup>10</sup> The advantage of the method proposed here is that it would be a direct probe of the Majorana nature of the quasiparticles. Transverse gradients of the Majorana polarization, relative to the density, are an indication of a delocalization process that ultimately could be detrimental to the zero-energy modes.

This paper is organized as follows. In Sec. II we present the microscopic model and briefly outline methodological details. In Sec. III we investigate the spatial profiles and polarization of the Majorana modes, focusing on their evolution with respect to varying the width of the homogeneous metallic strip. Sec. V discusses the Majorana localization driven by a point-like electrostatic defect, and Sec. VI summarizes the main results.

## II. MICROSCOPIC MODEL

For a description of the planar Josephson heterostructure, see Fig. 1, we employ the microscopic scenario discussed in Refs. 26, 27, and 43. The model Hamiltonian,

$$\mathcal{H} = \mathcal{H}_0 + \mathcal{H}_Z + \mathcal{H}_S, \quad (1)$$

consists first of the free term

$$\mathcal{H}_0 = \sum_{\langle i,j \rangle} [\lambda(\mathbf{d}_{ij} \times \vec{\sigma}_{\sigma\sigma'})_z - t\delta_{\sigma\sigma'}] d_{i\sigma}^\dagger d_{j\sigma'} - \mu \sum_{i\sigma} d_{i\sigma}^\dagger d_{i\sigma} \quad (2)$$

describing itinerant electrons hopping all over the sample.  $t$  is the hopping integral between the nearest neighbor sites on a square lattice,  $\lambda$  is the strength of the Rashba spin-orbit coupling,  $\mathbf{d}_{ij}$  is the vector connecting nearest neighbors, and  $\sigma$  stands for the vector of the Pauli matrices. The second (Zeeman) term

$$\mathcal{H}_Z = B_0 \sum_i \sum_{\sigma\sigma'} d_{i\sigma}^\dagger \sigma_{\sigma\sigma'}^x d_{i\sigma'} \quad (3)$$

accounts for the influence of an external magnetic field  $B_0$  which is parallel to the interface between the metallic and

superconducting regions, as reported experimentally.<sup>28,29</sup> The last part appearing in the model Hamiltonian (1) describes the on-site pairing in the left ( $S_L$ ) and right ( $S_R$ ) superconducting regions,

$$\mathcal{H}_S = \sum_i \left( \Delta_i d_{i\downarrow}^\dagger d_{i\uparrow}^\dagger + \text{H.c.} \right), \quad (4)$$

where

$$\Delta_i = \begin{cases} \Delta e^{-i\phi/2} & \text{for } i \in S_L, \\ \Delta e^{i\phi/2} & \text{for } i \in S_R, \text{ and} \\ 0 & \text{for } i \in N. \end{cases} \quad (5)$$

Here the metallic strip region is denoted by  $N$ . The phase difference between the superconducting layers  $S_R$  and  $S_L$  is  $\phi$  and  $\Delta$  is real.

We studied the finite-size version of this model, consisting of  $N_x$  sites along  $x$ -direction and  $N_y$  sites along  $y$ -axis. For specific computations we assumed  $N_x = 91$  and  $N_y = 30$ , unless stated otherwise. The eigenstates and eigenenergies of the heterostructure were determined numerically, solving the Bogoliubov de-Gennes equations with the canonical transformation

$$\begin{pmatrix} d_{i\uparrow} \\ d_{i\downarrow}^\dagger \end{pmatrix} = \sum_n \begin{bmatrix} u_{i\uparrow}^n & (v_{i\downarrow}^n)^* \\ -v_{i\downarrow} & (u_{i\uparrow}^n)^* \end{bmatrix} \begin{pmatrix} \gamma_n \\ \gamma_n^\dagger \end{pmatrix}, \quad (6)$$

where  $\gamma_n^{(\dagger)}$  stand for the Bogoliubov quasiparticles which diagonalize the Hamiltonian:  $H = \sum_n E_n \gamma_n^\dagger \gamma_n + \text{const.}$

In particular we have calculated the local density of states

$$\rho_i(\omega) = \sum_{n,\sigma} (|u_{i\sigma}^n|^2 \delta(\omega - E_n) + |v_{i\sigma}^n|^2 \delta(\omega + E_n)). \quad (7)$$

As we consider a finite size system we have broadened the delta function peaks to Lorentzian functions of width  $0.02\Delta$ .

Another quantity of interest is the Majorana polarization<sup>21,38</sup> for an eigenstate  $|\psi_n\rangle$ ,

$$\mathcal{P}_{in} = \langle \psi_n | \mathcal{C} \hat{r}_i | \psi_n \rangle = \sum_{\sigma} \sigma_{\sigma\sigma}^z 2u_{i\sigma}^n v_{i\sigma}^n, \quad (8)$$

where  $\hat{r}_i$  is projection onto site  $i$  and  $\mathcal{C}$  is the particle-hole operator. This quantity allows one to probe directly the Majorana nature of the eigenstates, and its experimental measurement is discussed in Sec. III B. For convenience we introduce

$$\mathcal{P}_i = \mathcal{P}_{i\uparrow} - \mathcal{P}_{i\downarrow} \quad (9)$$

where

$$\mathcal{P}_{i\sigma} = 2u_{i\sigma}^{n_0} v_{i\sigma}^{n_0}. \quad (10)$$

for the zero-energy ( $n = n_0$ ) quasiparticles. More generally one may wish to consider the particle-hole overlap  $u_{i\sigma_1}^n v_{j\sigma_2}^m$ . In particular the equal-spin pairing ( $\sigma_1 = \sigma_2$ ) induced between the neighboring sites  $i$  and  $j$  for the zero-energy quasiparticles ( $E_n = 0 = E_m$ ) is of interest. More details on this issue are discussed in Sec. III B.

### III. TOPOGRAPHY OF MAJORANA MODES

Upon substituting the metallic strip between the superconducting reservoirs, their Cooper pairs leak into the normal region, inducing on-site electron pairing. This proximity effect is efficient nearby the bulk superconductors, up to distances smaller than the coherence length  $\xi$ . Here we consider metallic samples comprising a few  $N_w$  atomic rows, whose spatial width  $N_w a \leq \xi$ , where  $a$  is the inter-atomic distance. Under such a condition the proximity effect induces superconductivity across the entire metallic region. The appearance of the topological superconducting phase, however, can be realized only with triplet pairing which can be achieved by combining conventional superconductivity with the spin-orbit Rashba interaction and Zeeman splitting.<sup>5</sup>

It has been demonstrated<sup>26,27</sup> that a transition from the topologically trivial to the nontrivial superconducting state is sensitive to the Josephson phase  $\phi$ . Characteristic features of the emerging Majorana quasiparticles can, however, additionally depend on the width  $N_w a$  of the metallic strip. In what follows we analyze such qualitative changes and propose a method for their empirical detection (Sec. IV).

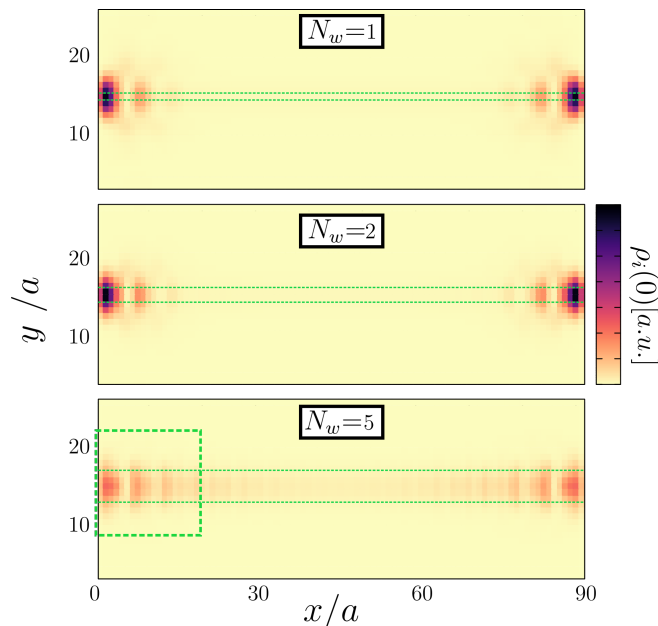


FIG. 2. The spatial profiles,  $\rho_i(0)$ , of the Majorana quasiparticles appearing in a metallic strip consisting of 1, 2 and 5 rows of atomic chains, as indicated. We have used the model parameters  $\Delta = 0.25t$ ,  $\phi = \pi$ ,  $\lambda = 0.5t$ ,  $B_0 = 0.1t$ ,  $\mu = -3.75t$ . The Majorana polarization (10) for the area in the green square is shown in Fig. 3.

### A. Zero-energy spectral function

Focusing on the optimal condition for the topological superconducting state  $\phi = \pi$ , we have checked that the on-site pairing  $\langle d_{i\downarrow} d_{i\uparrow} \rangle$  spreads nearly uniformly onto the metallic strip, both along and across it. Furthermore, we also noticed some feedback of the metallic sector onto superconducting regions manifested by partial reduction of the local pairing (sometimes referred to as the inverse superconducting proximity effect). Next, when combined with the spin-orbit interaction and the Zeeman field, the proximitized metallic stripe develops inter-site pairing of identical spin electrons, i.e. triplet pairing. For sufficiently strong magnetic fields  $B_0$ , such a triplet superconducting phase becomes topologically nontrivial, leading to the emergence of the zero-energy quasiparticles.<sup>26,27</sup>

Fig. 2 displays the spatial profiles of the local density of states at zero energy  $\rho_i(0)$ , obtained for very narrow metallic strips. We note that the Majorana quasiparticles of the narrow metallic strip are well localized at its ends. Their overall topography is practically identical with all features of one-dimensional systems, including the characteristic oscillations along the metallic strip.<sup>44</sup> It comes as perhaps some surprise that this narrow width of metallic region is neither essential for the development of the topological superconducting phase, nor important for the spatial profile of the Majorana modes. Even in the extreme case  $N_w = 0$ , i.e. without any metallic piece between the phase-differing superconductors, such modes are still present. On the other hand, when the width  $N_w$  increases we see a gradual smearing of the zero-energy quasiparticles and novel features appearing in the Majorana polarization. This is a consequence of the reduced proximity induced gap in wider strips which naturally reduces the localization of any mid-gap states.

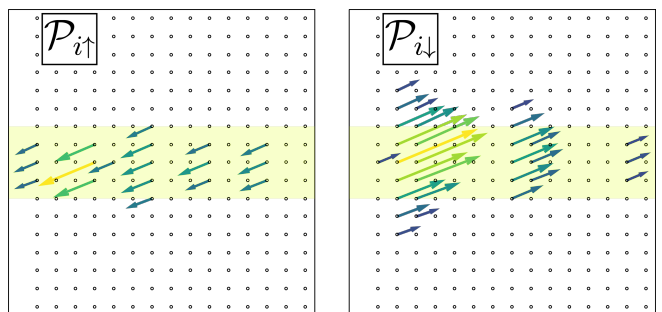


FIG. 3. Components of the Majorana polarization  $\mathcal{P}_{i\sigma}$  obtained for the region highlighted by the dashed frame in Fig. 2. The magnitude of the arrows shows  $|\mathcal{P}_{i\sigma}|$  and their direction shows  $\text{Arg } \mathcal{P}_{i\sigma}$ . We note that the phase of the Majorana polarization is only well defined up to a global shift. The shaded region is the metallic strip.

## B. Majorana polarization

Majorana modes are quasiparticles with energy  $E_n = 0$  (we denote such doubly-degenerate eigenstate by  $n \equiv n_0$ ) and which are eigenstates of the particle-hole transformation operator. We analyze here another valuable source of information about these modes encoded in the Majorana polarization.<sup>37–39,45</sup> This quantity is particularly useful for characterizing the Majorana modes of quasi two-dimensional topological superconductors<sup>21,38,41</sup> where its phase develops both longitudinal and transverse variation. As we shall see, its texture brings an important message about the delocalized Majorana quasiparticles.

Let us start by checking the contributions  $\mathcal{P}_{i\sigma}$  from each spin  $\sigma$  to the Majorana polarization in the narrow metallic strips, when the zero-energy quasiparticles are well localized near its ends. To be specific, we focus on the region marked by the dashed lines in the bottom panel in Fig. 2. Both constituents  $\mathcal{P}_{i\sigma}$  are depicted in Fig. 3 on the lattice sites of the marked metallic region. We clearly note that the directions of the arrows depicting  $\mathcal{P}_{i\uparrow}$  are opposite to  $\mathcal{P}_{i\downarrow}$ , which is typical for both strictly one-dimensional topological superconductors (see Fig. 2 in Ref. 40) and for higher dimensions as well.<sup>21,38,41</sup> The magnitudes of the two components, shown by the length of the arrows, are however very different. It is important to emphasize, that for the realization of a true MBS the local phase of  $\mathcal{P}_{i\uparrow} - \mathcal{P}_{i\downarrow}$  must be constant. Such a constraint  $\mathcal{P}_{i\uparrow} = e^{i\varphi}|\mathcal{P}_{i\uparrow}| = -e^{i\varphi}|\mathcal{P}_{i\downarrow}|$  seems to be satisfied in our case only for narrow metallic strips.

There are in fact two conditions on  $\mathcal{P}_i$  which are required for Majorana modes. The first, which we have seen here, is that its phase must be constant. The phase of  $\mathcal{P}_i$  does not appear to be measurable in any simple way. What is measurable, as we will show in Sec. IV, is its magnitude  $|\mathcal{P}_i|$ . For a Majorana mode we require  $|\mathcal{P}_i| = \rho_i^0$ , and this gives a measurable determination of Majorana modes. Upon increasing the width of the metallic strip the Majorana polarization gradually develops varying orientations, both along and across the sample. Emergence of the transverse gradient is very sensitive to the width  $N_w$ , as illustrated in Fig. 4.

## IV. POLARIZED ANDREEV SPECTROSCOPY

Here we briefly discuss an empirical method based on spin polarized Andreev reflection spectroscopy,<sup>42</sup> which could probe the absolute value of the Majorana polarization. Let us consider a scanning tunnelling microscope (STM) tip approaching site  $i$  of our heterostructure. The influence of this external reservoir of itinerant electrons can be incorporated by augmenting the model Hamilto-

nian Eq. (1) with the local term

$$H_i = \underbrace{\sum_{\mathbf{k},\sigma} (\varepsilon_{\mathbf{k}} - \mu_{tip}) c_{\mathbf{k}\sigma}^\dagger c_{\mathbf{k}\sigma}}_{\text{STM tip}} + \underbrace{\sum_{\mathbf{k},\sigma} (\gamma_{\mathbf{k},\sigma} c_{\mathbf{k}\sigma}^\dagger d_{i\sigma} + H.c.)}_{\text{hybridization}}, \quad (11)$$

where the chemical potential of the tip,  $\mu_{tip} = \mu + eV$ , can be varied by an applied bias voltage  $V$ .  $\varepsilon_{\mathbf{k}}$  is the dispersion of the tip electrons, and  $\gamma_{\mathbf{k}}$  the tunneling amplitude from the tip to the heterostructure and vice-versa. The quasiparticle spectrum at site  $i$  can be indirectly deduced from measurements of the charge transport induced by the voltage  $V$  applied between the STM tip and the sample. In the subgap regime, i.e. for  $e|V| \leq \Delta$ , such a current would solely originate from Andreev scattering processes. This mechanism relies on the conversion of electrons arriving from the STM tip into the Cooper pairs of the superconducting heterostructure, with holes being reflected back into the STM tip.

We are interested here in probing the topological superconducting phase related to the  $p$ -wave pairing of equal spin electrons induced between neighboring sites, analogous to the situation in Kitaev's simple model.<sup>46</sup> For this purpose let us assume a complete polarization of the tip, where only one spin component  $\sigma$  can participate in the charge transport. On a microscopic level we thus imagine that an itinerant electron of spin  $\sigma$  arrives from the polarized STM tip at site  $i$  where it forms a triplet pair with an electron from the neighbouring site  $j$ , sending a hole of the same spin orientation into the tip. Within the Landauer formalism we can express the resulting spin-dependent charge current by<sup>40</sup>

$$I_{ij}^\sigma(V) = \frac{e}{h} \int d\omega T_{ij}^\sigma(\omega) [f(\omega - eV) - f(\omega + eV)], \quad (12)$$

where  $f(\omega) = [1 + \exp(\omega/k_B T)]^{-1}$  is the Fermi-Dirac distribution function. The main quantities of interest are the spatially-dependent transmission probabilities<sup>40</sup>

$$T_{ij}^\sigma(\omega) = \Gamma_N^2 |\mathcal{F}_{ij}^\sigma(\omega)|^2, \quad (13)$$

where  $\mathcal{F}_{ij}^\sigma(\omega) = \langle\langle \hat{a}_{i\sigma}; \hat{d}_{j\sigma} \rangle\rangle_\omega$  is the Fourier transform of the anomalous retarded Green's function in Nambu representation. For practical reasons, because we focus on a small charge transport window which is only a fraction of meV around the chemical potential  $\mu$  of our sample, we have introduced a constant coupling strength,  $\Gamma_N \equiv 2\pi \sum_{\mathbf{k}} |\gamma_{\mathbf{k}}|^2 \delta(\omega - \varepsilon_{\mathbf{k}})$ . Formally it is equivalent to the wide band limit approximation.

The anomalous Green's function  $\mathcal{F}_{ij}^\sigma(\omega)$  has the explicit form, for  $\sigma = \uparrow$ ,

$$\mathcal{F}_{ij}^\uparrow(\omega) = - \sum_n \left[ \frac{u_{i\uparrow}^n (v_{j\uparrow}^n)^*}{\omega + i\Gamma_N - E_n} + \frac{u_{j\uparrow}^n (v_{i\uparrow}^n)^*}{\omega + i\Gamma_N + E_n} \right], \quad (14)$$

where  $u_{j\uparrow}^n$  and  $v_{j\uparrow}^n$  can be computed numerically.

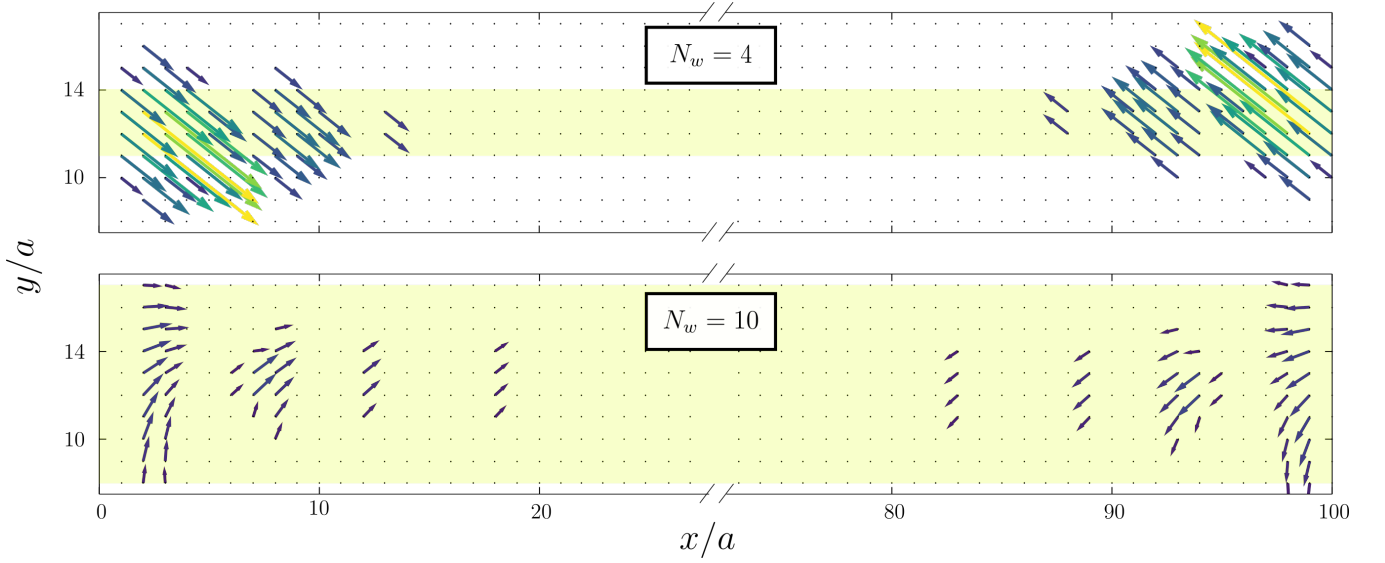


FIG. 4. The Majorana polarization  $\mathcal{P}_i$  obtained for the heterostructure comprising  $N_w = 4$  (top) and  $N_w = 10$  (bottom) atomic rows in the metallic strip, marked by the shaded region. Numerical results are obtained for the same model parameters as in Fig. 2 but using  $N_x = 100$ ,  $N_y = 20$ . The magnitude of the arrows shows  $|\mathcal{P}_{i\sigma}|$  and their direction shows  $\text{Arg } \mathcal{P}_{i\sigma}$ . We note that the phase is only well defined up to a global shift.

Focusing on the zero-energy limit  $\omega \rightarrow 0$ , dominated by the Andreev scatterings via the Majorana quasiparticle ( $E_{n_0} = 0$ ), we can express the transmittance by

$$T_{ij}^\sigma(\omega \sim 0) \simeq \frac{\Gamma_N^2}{\omega^2 + \Gamma_N^2} \left| u_{i\sigma}^{n_0} (v_{j\sigma}^{n_0})^* + u_{j\sigma}^{n_0} (v_{i\sigma}^{n_0})^* \right|^2. \quad (15)$$

Substituting Eq. (15) into the Andreev current formula (12) yields, at low temperatures, the following zero-bias differential conductance

$$\lim_{V \rightarrow 0} \frac{dI_{ij}^\sigma(V)}{dV} \simeq \frac{4e^2}{h} \left| u_{i\sigma}^{n_0} (v_{j\sigma}^{n_0})^* + u_{j\sigma}^{n_0} (v_{i\sigma}^{n_0})^* \right|^2. \quad (16)$$

This result (16) demonstrates that selective Andreev transport might probe the spin-dependent contribution (10) to the Majorana polarization. Strictly speaking, however, such tunneling processes occur on the links (involving the neighbouring sites  $i$  and  $j$ ) rather than on individual local sites. For this reason the differential conductance (16) would measure the *symmetrized Majorana polarization*

$$\mathcal{P}_{\langle ij \rangle, \sigma} = u_{i\sigma}^{n_0} v_{j\sigma}^{n_0} + u_{j\sigma}^{n_0} v_{i\sigma}^{n_0} \quad (17)$$

over the neighboring sites  $i$  and  $j$ , instead of the strictly local definition (10). Since the diagonalization coefficients are slowly varying in space,  $u_{j\sigma}^n \approx u_{i\sigma}^n$ ,  $v_{j\sigma}^n \approx v_{i\sigma}^n$ , the symmetrized  $\mathcal{P}_{\langle ij \rangle, \sigma}$  and local  $\mathcal{P}_{i, \sigma}$  Majorana polarizations should in practice be nearly identical.

Let us finally recall that the complex vector  $u_{i\uparrow}^{n_0} v_{i\uparrow}^{n_0}$  is typically perfectly opposite to  $u_{i\downarrow}^{n_0} v_{i\downarrow}^{n_0}$ , see Fig. 3. This implies, that the absolute value of the Majorana polarization (9)  $|\mathcal{P}_i| = |\mathcal{P}_{i\uparrow}| + |\mathcal{P}_{i\downarrow}|$ , and the same holds for the symmetrized Majorana polarization.

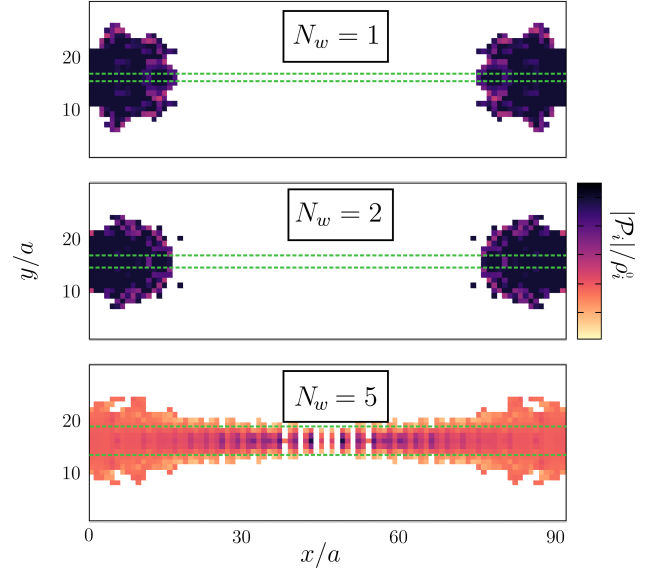


FIG. 5. The spatial profile of  $|\mathcal{P}_i|/\rho_i^0$  for the potential zero-energy Majorana quasiparticles appearing in the metallic strip consisting of 1, 2 and 5 rows of atomic chains, as indicated. We have used the same model parameters as in Fig. 2:  $\Delta = 0.25t$ ,  $\phi = \pi$ ,  $\lambda = 0.5t$ ,  $B_0 = 0.1t$ ,  $\mu = -3.75t$ . The difference between the well isolated MBS and the delocalized states in the wider strip is evident.

In conclusion, by measuring the zero-bias differential conductance  $\frac{dI_{ij}^\sigma(0)}{dV}$  of the spin-selective Andreev current flowing through the neighboring sites  $i$  and  $j$  one can evaluate the absolute value of the symmetrized Majorana

polarization

$$|\mathcal{P}_{\langle ij \rangle}| = \sqrt{\frac{\hbar}{4e^2}} \sqrt{\frac{d}{dV} [I_{ij}^\uparrow(0) + I_{ij}^\downarrow(0)]}. \quad (18)$$

As far as the spatial variation of the phase is concerned, its determination is, if possible, evidently more cumbersome. This problem is beyond the scope of the present study.

Although the spatial variation of the phase is not currently measurable we can compare the absolute value of  $|\mathcal{P}_i|$  with  $\rho_i(0)$ . For a MBS these must be the same, therefore if we plot the ratio of these measurable quantities,  $|\mathcal{P}_i|/\rho_i(0)$ , it should be flat for a MBS. In Fig. 5 we show results for  $N_w \in \{1, 2, 5\}$ , comparable to Fig. 2, which show that the MBS profile is indeed flat. For  $N_w = 5$ , when the two MBS at either end of the strip start to overlap, this quantity is no longer flat. Thus this can be used as an experimental determination of whether localized states are actually MBS. It is worth noting that increasing the length  $N_x$  of the system would result in  $|\mathcal{P}_i|/\rho_i(0)$  being flat even for  $N_w > 5$ .

## V. LOCALIZATION OF THE MAJORANA MODES

In Sec. III we have shown that upon increasing the width  $N_w$  of a metallic strip the topological superconducting state reveals (i) smearing of the Majorana quasiparticle, and (ii) development of the transverse gradient of the Majorana polarization. One may ask, however, whether there is any chance of localization of the Majorana modes. In this section we illustrate that such an effect could be observable due to local defects introduced in certain regions of the metallic strip.

Topological superconductivity in 1-dimensional wires and atomic chains has been shown to be robust against weak disorder,<sup>47–54</sup> noise,<sup>55</sup> inhomogeneous spin-orbit coupling,<sup>56</sup> reorientation of the magnetic field,<sup>41,57</sup> and thermal fluctuations.<sup>58–61</sup> Sufficiently strong scattering centers, however, could effectively break these 1-dimensional systems into separate segments, inducing additional pairs of the Majorana modes.<sup>62</sup> Such a mechanism can be expected to be inefficient in 2-dimensional systems. To verify this conjecture for the quasi 2-dimensional heterostructure discussed in this paper we take into consideration a point-like electrostatic defect  $\mathcal{H}_{imp} = V_0 d_{i_0\sigma}^\dagger d_{i_0\sigma}$  positioned at site  $i_0$  of the metallic region. We assume this scattering potential to be rather strong,  $V_0 = 100t$ , as otherwise its influence would be less visible.

Let us first assume the scattering potential to be placed in a central part of the metallic region (Fig. 6(a)). Neither the zero-energy spectral function nor the Majorana polarization reveal any influence of such an electrostatic impurity on the existing Majorana quasiparticles, in contrast to the properties of 1-dimensional topological superconductors.<sup>62</sup> This behaviour seems to be quite natural,

because the Majorana modes are safely distant from the impurity.

Contrary to this situation, let us next consider the scattering potential near the left side of the metallic strip (Fig. 6(b,c)). We selected the specific sites  $i_0 = 4$  and  $i_0 = 8$ , in order to guarantee a considerable overlap of the local defect with the left hand Majorana mode. Under such circumstances the scattering potential has a substantial influence both on the spectral function (left panels) and the Majorana polarization (right panels). This electrostatic impurity reduces the spatial extent of the Majorana quasiparticle on the left hand side, whereas the other Majorana quasiparticle is practically left intact. Such a tendency towards localization of the Majorana modes has been recently predicted by Haim and Stern,<sup>36</sup> when investigating the different role of weak extended disorder.

Our present study provides more detailed information concerning such disorder-induced-localization, indicating that: (i) disorder present in the internal segments of the metallic strip would naturally be rather ineffective for the Majorana quasiparticles, whereas (ii) disorder introduced to the regions of already existing Majorana quasiparticles substantially reduces their spatial extent. The considerations discussed in Sec. IV suggest that empirical detection of this subtle phenomenon could be feasible. A tendency towards the localization of the Majorana quasiparticles could be observed in the maps of differential conductance for the spin polarized Andreev current induced via the metallic region in the presence of the intentionally deposited local defects. Such an electrostatic scattering potential could be created by applying gate potentials, whereas a magnetic potential, leading to similar effects, can be obtained by locally perturbing the Zeeman field.

## VI. SUMMARY

We have theoretically studied the properties of the Majorana quasiparticles emerging in a narrow metallic strip sandwiched between two *s*-wave superconductors in a Josephson-junction geometry. The topological superconducting phase has been recently reported for such metallic strips by the groups in Copenhagen<sup>28</sup> and Harvard<sup>29</sup> with a length-to-width ratio ranging from 20 to 100, respectively. Using the Bogoliubov de-Gennes treatment we have investigated the role of the finite metallic strip width, exploring its influence on: (a) spatial profiles of the zero-energy quasiparticles and (b) topography of the Majorana polarization that probes the particle-hole overlap of the zero-energy quasiparticles. Furthermore, we have proposed a feasible method for detecting the magnitude of such a Majorana polarization by measuring the differential conductance in spin-polarized Andreev reflection spectroscopy.

We have also analyzed the influence of strong (point-like) electrostatic defects on the Majorana modes. We

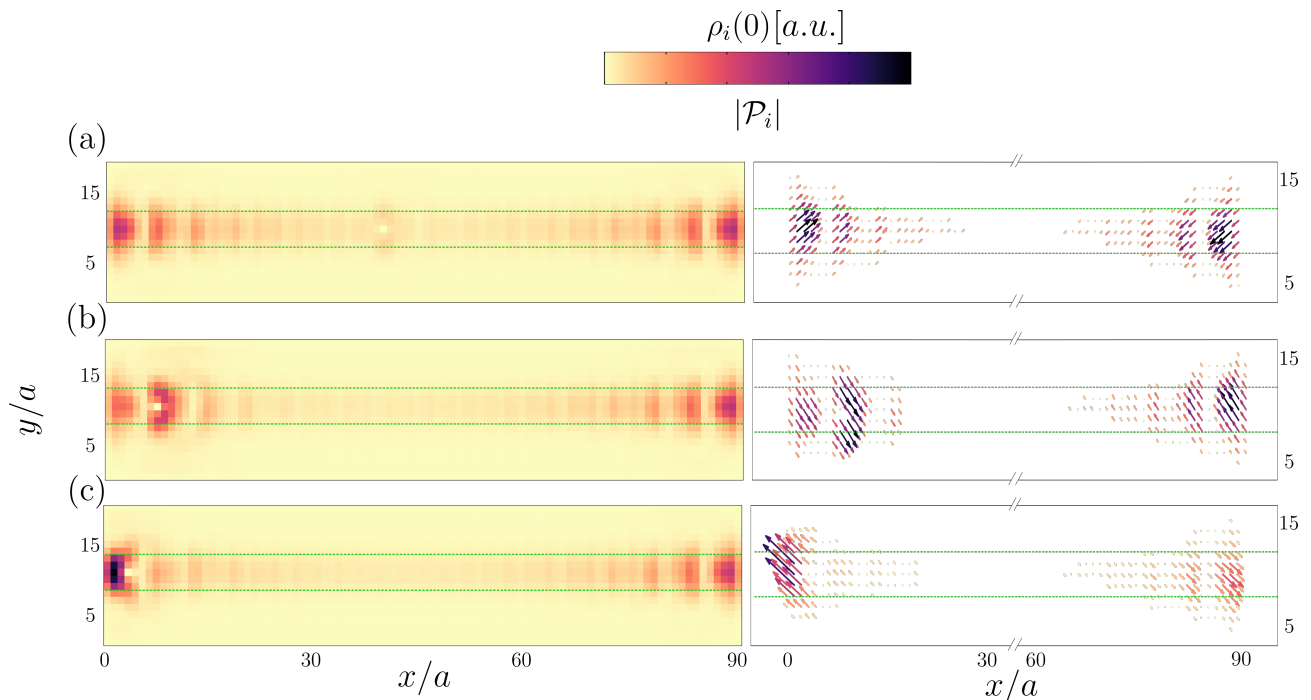


FIG. 6. The spatial density profile of the zero-energy Majorana quasiparticles (left panels) and their polarizations (right panels) obtained in the proximitized metallic strip, consisting of  $N_w = 5$  rows of atoms, in presence of a point-like electrostatic defect with  $V_0 = 100t$  at site: (a)  $i_0 = 40a$ , (b)  $i_0 = 8a$ , and (c)  $i_0 = 4a$  and  $N_y = 20$ . The magnitude of the arrows in the right hand side plots show  $|\mathcal{P}_{i\sigma}|$  and their direction show  $\text{Arg } \mathcal{P}_{i\sigma}$ . We note that the phase is only well defined up to a global shift.

have revealed that such a local scattering potential can affect the localization length of the Majorana quasiparticles if deposited near the ends of the metallic strip. Under such circumstances the neighboring Majorana mode substantially reduces its spatial extent, which can be compared with what has been predicted in Ref.,<sup>36</sup> whereas the opposite-end Majorana mode remains practically intact. Similar coexistences of the localized and delocalized Majorana quasiparticles have been previously observed by scanning tunneling spectroscopy using a disordered monolayer of superconducting *Pb* coupled to underlying *Co* – *Si* magnetic islands.<sup>22</sup> We hope that proximitized metallic strips would be a convenient platform not only for the realization of topological superconductivity, tunable by the magnetic field and Josephson phase, but could also allow for manipulating the Majorana quasiparticle length-scale.

#### ACKNOWLEDGMENTS

We thank Benedikt Scharf for instructive discussions. This work is supported by National Science Centre (Poland) under the grants UMO-2017/27/N/ST3/01762 (SG), UMO-2018/29/B/ST3/01892 (NS), and UMO-2018/29/B/ST3/00937 (TD).

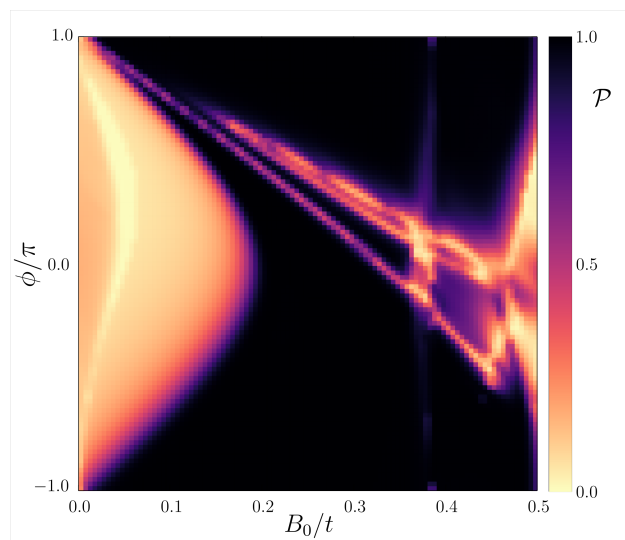


FIG. 7. The topological superconducting phase (dark area) with respect to the magnetic field  $B_0$  and the Josephson phase  $\phi$  obtained by the criterion concerning the global Majorana polarization.<sup>21,38</sup> Numerical computations were done for  $N_w = 2$  and the same model parameters as in Fig. 2.

## Appendix: Influence of the Josephson phase

In the main part of this manuscript we have analyzed the spectroscopic properties of the Majorana quasiparticles, focusing on the particular case  $\phi = \pi$ , that is optimal for occurrence of the topological superconducting state. Similar qualitative features would be also observable for other values of the Josephson phase  $\phi \neq \pi$ , provided that model parameters (such as, e.g., the magnetic field) are appropriately tuned.<sup>26,27</sup> A possible criterion (proposed by one of us<sup>21,38</sup>) for determination of the topological diagram relies on the Majorana polarization for MBS to be non-vanishing when summed over a portion of the investigated system where the bound states should reside, in fact it should be equal to the total den-

sity of the state in the same region. Therefore

$$\mathcal{P} = \sum_{i \in \mathcal{R}} \frac{|\mathcal{P}_{i n_0}|}{\rho_i(E_{n_0})} = 1 \quad (\text{A.1})$$

for a MBS. This serves as a proxy for being in the topologically non-trivial phase. In the present scenario one can choose for this purpose either the leftmost or rightmost quarter of the metallic strip as the region  $\mathcal{R}$ . More details can be found in Ref. 21.

Fig. 7 displays the topological phase diagram, with the dark area being the nontrivial phase, obtained using this criterion for our heterostructure. We show the phase diagram with respect to the magnetic field  $B_0$  and the Josephson phase  $\phi$ . Let us remark, that such a criterion yields a smooth changeover between the topologically trivial and nontrivial superconducting states instead of a sharp transition. It can be hence useful for exploring the robustness of the topological state against perturbations such as inhomogeneity or thermal fluctuations.

\* e-mail: [szglodzik@kft.umcs.lublin.pl](mailto:szglodzik@kft.umcs.lublin.pl)

† e-mail: [sedlmayr@umcs.pl](mailto:sedlmayr@umcs.pl)

‡ e-mail: [doman@kft.umcs.lublin.pl](mailto:doman@kft.umcs.lublin.pl)

<sup>1</sup> M. T. Deng, C. L. Yu, G. Y. Huang, M. Larsson, P. Caroff, and H. Q. Xu, “Anomalous zero-bias conductance peak in a Nb–InSb nanowire–Nb hybrid device,” *Nano Lett.* **12**, 6414 (2012).

<sup>2</sup> V. Mourik, K. Zuo, S. M. Frolov, S. R. Plissard, E. P. A. M. Bakkers, and L. P. Kouwenhoven, “Signatures of Majorana fermions in hybrid superconductor-semiconductor nanowire devices,” *Science* **336**, 1003 (2012).

<sup>3</sup> A. Das, Y. Ronen, Y. Most, Y. Oreg, M. Heiblum, and H. Shtrikman, “Zero-bias peaks and splitting in an Al–InAs nanowire topological superconductor as a signature of Majorana fermions,” *Nat. Phys.* **8**, 887 (2012).

<sup>4</sup> A. D. K. Finck, D. J. Van Harlingen, P. K. Mohseni, K. Jung, and X. Li, “Anomalous modulation of a zero-bias peak in a hybrid nanowire-superconductor device,” *Phys. Rev. Lett.* **110**, 126406 (2013).

<sup>5</sup> R. M. Lutchyn, E. P. A. M. Bakkers, L. P. Kouwenhoven, P. Krogstrup, C. M. Marcus, and Y. Oreg, “Majorana zero modes in superconductor-semiconductor heterostructures,” *Nat. Rev. Mater.* **3**, 52 (2018).

<sup>6</sup> S. Nadj-Perge, I. K. Drozdov, J. Li, H. Chen, S. Jeon, J. Seo, A. H. MacDonald, B. A. Bernevig, and A. Yazdani, “Observation of Majorana fermions in ferromagnetic atomic chains on a superconductor,” *Science* **346**, 602 (2014).

<sup>7</sup> R. Pawlak, M. Kisiel, J. Klinovaja, T. Meier, S. Kawai, T. Glatzel, D. Loss, and E. Meyer, “Probing atomic structure and Majorana wavefunctions in mono-atomic Fe chains on superconducting Pb surface,” *Npj Quantum Information* **2**, 16035 (2016).

<sup>8</sup> B. E. Feldman, M. T. Randeria, J. Li, S. Jeon, Y. Xie, Z. Wang, I. K. Drozdov, B. A. Bernevig, and A. Yazdani, “High-resolution studies of the Majorana atomic chain

platform,” *Nat. Phys.* **13**, 286 (2016).

<sup>9</sup> M. Ruby, B. W. Heinrich, Y. Peng, F. von Oppen, and K. J. Franke, “Exploring a proximity-coupled Co chain on Pb (110) as a possible Majorana platform,” *Nano Lett.* **17**, 4473 (2017).

<sup>10</sup> S. Jeon, Y. Xie, J. Li, Z. Wang, B. A. Bernevig, and A. Yazdani, “Distinguishing a Majorana zero mode using spin-resolved measurements,” *Science* **358**, 772 (2017).

<sup>11</sup> H. Kim, A. Palacio-Morales, T. Posske, L. Rózsa, K. Palotás, L. Szunyogh, M. Thorwart, and R. Wiesendanger, “Toward tailoring Majorana bound states in artificially constructed magnetic atom chains on elemental superconductors,” *Sci. Adv.* **4** (2018), 10.1126/sciadv.1701476.

<sup>12</sup> F. Nichele, A. C. C. Drachmann, A. M. Whiticar, E. C. T. O’Farrell, H. J. Suominen, A. Fornieri, T. Wang, G. C. Gardner, C. Thomas, A. T. Hatke, P. Krogstrup, M. J. Manfra, K. Flensberg, and Ch. M. Marcus, “Scaling of Majorana zero-bias conductance peaks,” *Phys. Rev. Lett.* **119**, 136803 (2017).

<sup>13</sup> J. Röntynen and T. Ojanen, “Topological superconductivity and high Chern numbers in 2D ferromagnetic Shiba lattices,” *Phys. Rev. Lett.* **114**, 236803 (2015).

<sup>14</sup> K. Björnson, S. S. Pershoguba, A. V. Balatsky, and A. M. Black-Schaffer, “Spin-polarized edge currents and Majorana fermions in one- and two-dimensional topological superconductors,” *Phys. Rev. B* **92**, 214501 (2015).

<sup>15</sup> J. Li, T. Neupert, Z. Wang, A. H. MacDonald, A. Yazdani, and B. A. Bernevig, “Two-dimensional chiral topological superconductivity in Shiba lattices,” *Nat. Commun.* **7**, 12297 (2016).

<sup>16</sup> S. Rachel, E. Mascot, S. Cocklin, M. Vojta, and D. K. Morr, “Quantized charge transport in chiral Majorana edge modes,” *Phys. Rev. B* **96**, 205131 (2017).

<sup>17</sup> Y. Volpez, D. Loss, and J. Klinovaja, “Rashba sandwiches with topological superconducting phases,” *Phys. Rev. B*

- 97**, 195421 (2018).
- 18 G. C. Ménard, S. Guissart, Ch. Brun, R. T. Leriche, M. Trif, F. Debontridder, D. Demaille, D. Roditchev, P. Simon, and T. Cren, “Two-dimensional topological superconductivity in Pb/Co/Si(111),” *Nat. Commun.* **8**, 2040 (2017).
  - 19 Q. L. He, L. Pan, A. L. Stern, E. C. Burks, X. Che, G. Yin, J. Wang, B. Lian, Q. Zhou, E. S. Choi, K. Murata, X. Kou, Z. Chen, T. Nie, Q. Shao, Y. Fan, S.-C. Zhang, K. Liu, J. Xia, and K. L. Wang, “Chiral Majorana fermion modes in a quantum anomalous Hall insulator–superconductor structure,” *Science* **357**, 294 (2017).
  - 20 A. Palacio-Morales, E. Mascot, S. Cocklin, H. Kim, S. Rachel, D.K. Morr, and R. Wiesendanger, “Atomic-scale interface engineering of Majorana edge modes in a 2D magnet-superconductor hybrid system,” *Sci. Adv.* **5**, eaav6600 (2019).
  - 21 N. Sedlmayr, J. M. Aguiar-Hualde, and C. Bena, “Majorana bound states in open quasi-one-dimensional and two-dimensional systems with transverse Rashba coupling,” *Phys. Rev. B* **93**, 155425 (2016).
  - 22 G. Ménard, A. Mesaros, C. Brun, F. Debontridder, D. Roditchev, P. Simon, and T. Cren, “Isolated pairs of Majorana zero modes in a disordered superconducting lead monolayer,” *Nat. Commun.* **10**, 2587 (2019).
  - 23 F. Nichele, A. C. C. Drachmann, A. M. Whiticar, E. C. T. O’Farrell, H. J. Suominen, A. Fornieri, T. Wang, G. C. Gardner, C. Thomas, A. T. Hatke, P. Krogstrup, M. J. Manfra, K. Flensberg, and C. M. Marcus, “Scaling of Majorana zero-bias conductance peaks,” *Phys. Rev. Lett.* **119**, 136803 (2017).
  - 24 A. Kobińska, A. Ptok, and T. Domański, “Delocalisation of Majorana quasiparticles in plaquettenanowire hybrid system,” *Sci. Rep.* **9**, 12933 (2019).
  - 25 E. Mascot, S. Cocklin, S. Rachel, and D.K. Morr, “Dimensional tuning of Majorana fermions and real space counting of the Chern number,” *Phys. Rev. B* **100**, 184510 (2019).
  - 26 F. Pientka, A. Keselman, E. Berg, A. Yacoby, A. Stern, and B.I. Halperin, “Topological superconductivity in a planar Josephson junction,” *Phys. Rev. X* **7**, 021032 (2017).
  - 27 Michael Hell, Martin Leijnse, and Karsten Flensberg, “Two-dimensional platform for networks of Majorana bound states,” *Phys. Rev. Lett.* **118**, 107701 (2017).
  - 28 A. Fornieri, A.M. Whiticar, F. Setiawan, E. Portoles, A.C.C. Drachmann, A. Keselman, S. Gronin, C. Thomas, T. Wang, R. Kallaher, G.C. Gardner, E. Berg, M.J. Manfra, A. Stern, Ch.M. Marcus, and F. Nichele, “Evidence of topological superconductivity in planar Josephson junctions,” *Nature* **569**, 89 (2019).
  - 29 H. Ren, F. Pientka, S. Hart, A.T. Pierce, M. Kosowsky, L. Lunczer, R. Schlereth, B. Scharf, E.M. Hankiewicz, L.W. Molenkamp, B.I. Halperin, and A. Yacoby, “Topological superconductivity in a phase-controlled Josephson junction,” *Nature* **569**, 93 (2019).
  - 30 W. Mayer, M.C. Dartiaillh, J. Yuan, A. Wickramasinghe, K.S. Matos-Abiague, I. Žutić, and J. Shabani, “Phase signature of topological transition in Josephson junctions,” (2019), [arXiv:1906.01179](https://arxiv.org/abs/1906.01179).
  - 31 F. Setiawan, Chien-Te Wu, and K. Levin, “Full proximity treatment of topological superconductors in Josephson-junction architectures,” *Phys. Rev. B* **99**, 174511 (2019).
  - 32 F. Setiawan, A. Stern, and E. Berg, “Topological superconductivity in planar Josephson junctions: Narrowing down to the nanowire limit,” *Phys. Rev. B* **99**, 220506 (2019).
  - 33 B. Scharf, F. Pientka, H. Ren, A. Yacoby, and E.M. Hankiewicz, “Tuning topological superconductivity in phase-controlled Josephson junctions with Rashba and Dresselhaus spin-orbit coupling,” *Phys. Rev. B* **99**, 214503 (2019).
  - 34 T. Laeven, B. Nijholt, M. Wimmer, and A.R. Akhmerov, “Enhanced proximity effect in zigzag-shaped Majorana Josephson junctions,” (2019), [arXiv:1903.06168](https://arxiv.org/abs/1903.06168).
  - 35 A. Stern and E. Berg, “Fractional Josephson vortices and braiding of Majorana zero modes in planar superconductor-semiconductor heterostructures,” *Phys. Rev. Lett.* **122**, 107701 (2019).
  - 36 A. Haim and A. Stern, “Benefits of weak disorder in one-dimensional topological superconductors,” *Phys. Rev. Lett.* **122**, 126801 (2019).
  - 37 D. Sticlet, C. Bena, and P. Simon, “Spin and Majorana polarization in topological superconducting wires,” *Phys. Rev. Lett.* **108**, 096802 (2012).
  - 38 N. Sedlmayr and C. Bena, “Visualizing Majorana bound states in one and two dimensions using the generalized Majorana polarization,” *Phys. Rev. B* **92**, 115115 (2015).
  - 39 N. Sedlmayr, G. Guigou, P. Simon, and C. Bena, “Majoranas with and without a ‘character’: hybridization, braiding and chiral Majorana number,” *J. Phys.: Condens. Matter* **27**, 455601 (2015).
  - 40 M. M. Maška and T. Domanski, “Polarization of the Majorana quasiparticles in the Rashba chain,” *Sci. Rep.* **7**, 16193 (2017).
  - 41 V. Kaladzhyan, J. Despres, I. Mandal, and C. Bena, “Majorana fermions in finite-size strips with in-plane magnetic fields,” *Eur. Phys. J. B* **90** (2017), [10.1140/epjb/e2017-80103-y](https://doi.org/10.1140/epjb/e2017-80103-y).
  - 42 J. J. He, T. K. Ng, P. A. Lee, and K. T. Law, “Selective equal-spin Andreev reflections induced by Majorana fermions,” *Phys. Rev. Lett.* **112**, 037001 (2014).
  - 43 B. Scharf, F. Pientka, H. Ren, A. Yacoby, and E.M. Hankiewicz, “Tuning topological superconductivity in phase-controlled Josephson junctions with Rashba and Dresselhaus spin-orbit coupling,” *Phys. Rev. B* **99**, 214503 (2019).
  - 44 D. Chevallier and J. Klinovaja, “Tomography of Majorana fermions with STM tips,” *Phys. Rev. B* **94**, 035417 (2016).
  - 45 N. Sedlmayr, J. M. Aguiar-Hualde, and C. Bena, “Flat Majorana bands in two-dimensional lattices with inhomogeneous magnetic fields: Topology and stability,” *Phys. Rev. B* **91**, 115415 (2015).
  - 46 A. Y. Kitaev, “Unpaired Majorana fermions in quantum wires,” *Phys.-Usp.* **44**, 131 (2001).
  - 47 P.W. Brouwer, M. Duckheim, A. Romito, and F. von Oppen, “Topological superconducting phases in disordered quantum wires with strong spin-orbit coupling,” *Phys. Rev. B* **84**, 144526 (2011).
  - 48 W. DeGottardi, D. Sen, and S. Vishveshwara, “Majorana fermions in superconducting 1d systems having periodic, quasiperiodic, and disordered potentials,” *Phys. Rev. Lett.* **110**, 146404 (2013).
  - 49 H.-Y. Hui, J.D. Sau, and S. Das Sarma, “Bulk disorder in the superconductor affects proximity-induced topological superconductivity,” *Phys. Rev. B* **92**, 174512 (2015).
  - 50 S. Hoffman, J. Klinovaja, and D. Loss, “Topological phases of inhomogeneous superconductivity,” *Phys. Rev. B* **93**, 165418 (2016).
  - 51 P. Zhang and F. Nori, “Majorana bound states in a disordered quantum dot chain,” *New J. Phys.* **18**, 043033 (2016).

- <sup>52</sup> Suraj S. Hegde and Smitha Vishveshwara, “Majorana wave-function oscillations, fermion parity switches, and disorder in kitaev chains,” *Phys. Rev. B* **94**, 115166 (2016).
- <sup>53</sup> W.S. Cole, J.D. Sau, and S. Das Sarma, “Proximity effect and Majorana bound states in clean semiconductor nanowires coupled to disordered superconductors,” *Phys. Rev. B* **94**, 140505 (2016).
- <sup>54</sup> B. Pekerten, A. Teker, Ö. Bozat, M. Wimmer, and İ. Adagideli, “Disorder-induced topological transitions in multichannel majorana wires,” *Phys. Rev. B* **95**, 064507 (2017).
- <sup>55</sup> Y. Hu, Z. Cai, M.A. Baranov, and P. Zoller, “Majorana fermions in noisy kitaev wires,” *Phys. Rev. B* **92**, 165118 (2015).
- <sup>56</sup> J. Klinovaja and D. Loss, “Fermionic and Majorana bound states in hybrid nanowires with non-uniform spin-orbit interaction,” *Eur. Phys. J. B* **88**, 62 (2015).
- <sup>57</sup> B. Kiczek and A. Ptok, “Influence of the orbital effects on the Majorana quasi-particles in a nanowire,” *J. Phys.: Condens. Matter* **29**, 495301 (2017).
- <sup>58</sup> J. Klinovaja, P. Stano, A. Yazdani, and D. Loss, “Topological superconductivity and Majorana fermions in RKKY systems,” *Phys. Rev. Lett.* **111**, 186805 (2013).
- <sup>59</sup> B. Braunecker and P. Simon, “Self-stabilizing temperature-driven crossover between topological and nontopological ordered phases in one-dimensional conductors,” *Phys. Rev. B* **92**, 241410 (2015).
- <sup>60</sup> W. Hu, R.T. Scalettar, and R. R. P. Singh, “Interplay of magnetic order, pairing, and phase separation in a one-dimensional spin-fermion model,” *Phys. Rev. B* **92**, 115133 (2015).
- <sup>61</sup> A. Gorczyca-Goraj, T. Domański, and M.M. Maška, “Topological superconductivity at finite temperatures in proximitized magnetic nanowires,” *Phys. Rev. B* **99**, 235430 (2019).
- <sup>62</sup> M. M. Maška, A. Gorczyca-Goraj, J. Tworzydło, and T. Domański, “Majorana quasiparticles of an inhomogeneous Rashba chain,” *Phys. Rev. B* **95**, 045429 (2017).